Estimation of the convergence order of rigorous coupled-wave analysis for OCD metrology

Yuan MA [a], Shiyuan LIU [*, a, b], Xiuguo CHEN [a], and Chuanwei ZHANG [b]

[a] Wuhan National Laboratory for Optoelectronics, Huazhong University of Science and Technology, Wuhan 430074, China;

[b] State Key Laboratory of Digital Manufacturing Equipment and Technology, Huazhong University of Science and Technology, Wuhan 430074, China

ABSTRACT

In most cases of optical critical dimension (OCD) metrology, when applying rigorous coupled-wave analysis (RCWA) to optical modeling, a high order of Fourier harmonics is usually set up to guarantee the convergence of the final results. However, the total number of floating point operations grows dramatically as the truncation order increases. Therefore, it is critical to choose an appropriate order to obtain high computational efficiency without losing much accuracy in the meantime. In this paper, the convergence order associated with the structural and optical parameters has been estimated through simulation. The results indicate that the convergence order is linear with the period of the sample when fixing the other parameters, both for planar diffraction and conical diffraction. The illuminated wavelength also affects the convergence of a final result. With further investigations concentrated on the ratio of illuminated wavelength to period, it is discovered that the convergence order decreases with the growth of the ratio, and when the ratio is fixed, convergence order jumps slightly, especially in a specific range of wavelength. This characteristic could be applied to estimate the optimum convergence order of given samples to obtain high computational efficiency.

Keywords: rigorous coupled-wave analysis, convergence order, optical modeling, nanometrology, critical dimension

1. INTRODUCTION

Generally, optical critical dimension (OCD) metrology consists of two parts in measuring the dimension of subwavelength structures, i.e., the forward modeling and the inverse problem[1]. Starting from Maxwell's equations, either in integrated or differential form, the electric and magnetic fields can be obtained in the forward modeling problem, from which we can further calculate the reflectivity or ellipsometric parameters[2-4]. Then in the inverse problem, the measured optical parameters are obtained and utilized to fit the simulation parameters using regression algorithms[5]. The forward modeling is repeated until the required accuracy is obtained and the structural parameters are measured to provide the best fit. Because this process takes time, it is highly desirable to improve the speed of optical modeling to achieve the greatest efficiency in OCD metrology.

Currently, the rigorous coupled-wave analysis (RCWA) method has been widely used in OCD metrology for the optical modeling of periodic structures[2, 6]. When implementing this technique, the permittivity of the grating region is first expanded into a series of Fourier harmonics, then the electromagnetic field is expressed as a Fourier expansion with a corresponding order of harmonics. In most cases when applying the RCWA technique for optical modeling, a high order of the Fourier harmonics is set up to make sure of the final convergence. However, the total number of floating point operations has a cubic relationship with the harmonic order[7]. This indicates that the technique will become rather time consuming if the expanded order is too high. Therefore, it is of great importance to choose an appropriate order to obtain high computational efficiency while maintaining sufficient accuracy.

In this paper, we aim at discovering the relationship between the convergence order and the structural or optical parameters, and providing guidance for the selection of an appropriate order when applying the RCWA technique. With a brief introduction of the RCWA theory in Section 2, we will present several simulations performed under different

* Contact author: shyliu@mail.hust.edu.cn; phone: +86 27 87792409; fax: +86 27 87792413; http://www2.hust.edu.cn/nom.

Seventh International Symposium on Precision Engineering Measurements and Instrumentation, edited by Kuang-Chao Fan, Rong-Sheng Lu, Man Song, Proc. of SPIE Vol. 8321
83211M · © 2011 SPIE · CCC code: /11/$18 · doi: 10.1117/12.904664

structural or optical conditions for binary rectangular groove gratings in Section 3. Finally, the estimations of the convergence order will be made for a few samples according to the observations.

2. THEORY FOR THE RIGOROUS COUPLED-WAVE ANALYSIS

Without losing the generality of the optical modeling, a binary rectangular groove grating is selected in our simulation, and its geometry is depicted in Fig. 1. Any multilayer structures with arbitrary profiles can be investigated on this basis[8]. A linearly monochromatic light is launched into the sample at a polar angle θ derived away from the z axis, and an azimuthal angle Φ between the plane of incidence and the grating vector along the direction normal to the walls. The angle ψ from the electric vector to the plane of incidence is called a polarized angle. Generally, this problem is named conical diffraction. When Φ approaches zero, which is called planar diffraction, the E-vector is normal (ψ=90°) and parallel (ψ=0°) to the plane of incidence for transverse electric (TE) and transverse magnetic (TM) polarization, respectively. The wavelength of the illuminated light in free space is λ_0. The refractive indices of superstrate and substrate are n_1 and n_2, respectively. The periods Λ are made up of ridges and grooves, in which the refractive indices are n_{rd} and n_{gr}, respectively. The materials of the resist and substrate layers are Si_3N_4 and silicon, respectively. f is the fraction of the grating period occupied by the resist, with the depth d along the z axis.

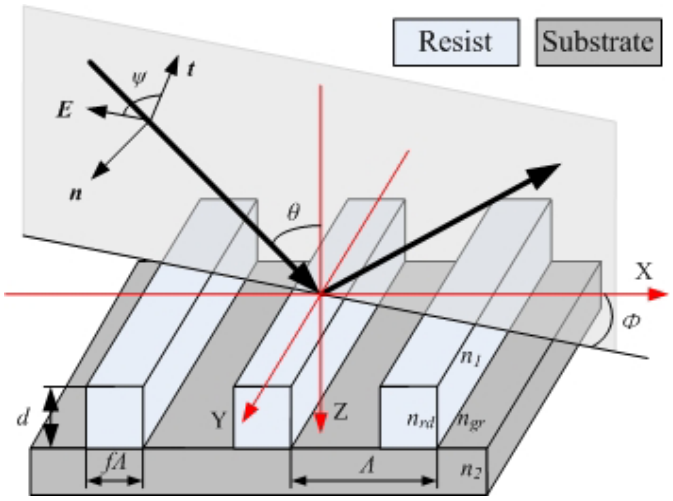

Figure 1. Geometry of the binary rectangular groove grating.

For TE polarization, the incident normalized electric field can be expressed as

$$E_{inc,y} = \exp\left[-jk_0 n_1 (\sin\theta\, x + \cos\theta\, z)\right], \tag{1}$$

where $k_0=2\pi/\lambda_0$. The Rayleigh expansions of the electric field of the reflected and transmitted region are

$$E_{\mathrm{I},y} = E_{inc,y} + \sum_i R_i \exp\left[-j(k_{xi}x - k_{\mathrm{I},zi}z)\right], \tag{2a}$$

$$E_{\mathrm{II},y} = \sum_i T_i \exp\left\{-j\left[k_{xi}x + k_{\mathrm{II},zi}(z-d)\right]\right\}, \tag{2b}$$

respectively, where k_{xi} can be determined from the Floquet condition and is given by

$$k_{xi} = k_0\left[n_1 \sin\theta - i(\lambda_0/\Lambda)\right], \tag{3}$$

and where $k_{m,zi}$ is calculated from the obtained k_0 and k_{xi}

$$k_{m,zi} = \begin{cases} +k_0\left[n_m{}^2 - (k_{xi}/k_0)^2\right]^{1/2} & k_0 n_m > k_{xi} \\ -jk_0\left[(k_{xi}/k_0)^2 - n_m{}^2\right]^{1/2} & k_{xi} > k_0 n_m \end{cases}, \; m = \mathrm{I}, \mathrm{II}. \tag{4}$$

It is always necessary to have in mind the physical meaning that the ith wave is propagating when $k_0 n_m > k_{xi}$, and evanescent when $k_x > k_0 n_m$. R_i and T_i are the normalized electric-field amplitudes of the ith reflected and transmitted wave, respectively.

The magnetic field in the reflected and transmitted region can be obtained from Maxwell's equations

$$\boldsymbol{H} = \left(\frac{j}{\omega\mu}\right)\nabla \times \boldsymbol{E}\,, \tag{5}$$

where μ is the permeability of the region and ω is the angular optical frequency.

In the grating region ($0<z<d$), equation (5) can be simplified in a scalar form as

$$\frac{\partial E_y}{\partial z} = j\omega\mu_0 H_x\,, \tag{6a}$$

$$\frac{\partial H_x}{\partial z} = j\omega \in_0 \varepsilon(x) E_y + \frac{\partial H_z}{\partial x}\,, \tag{6b}$$

where $\in_0$ is the permittivity of free space, and ε is the permittivity of the grating region and can be expanded in a Fourier form. The electric field along the y-axis and magnetic field along the x-axis may also be expressed with a Fourier expansion in terms of the space-harmonics field as

$$E_{gy} = \sum_i S_{yi}(z)\exp(-jk_{xi}x), \tag{7a}$$

$$H_{gx} = -j\left(\frac{\in_0}{\mu_0}\right)^{1/2}\sum_i U_{xi}(z)\exp(-jk_{xi}x), \tag{7b}$$

where $S_{yi}(z)$ and $U_{xi}(z)$ are the normalized amplitudes of the ith space-harmonic fields. Substituting equation (7) into equation (6), and eliminating H_z, we are able to obtain the coupled-wave equations as follows

$$\frac{\partial S_{yi}}{\partial z} = k_0 U_{xi}\,, \tag{8a}$$

$$\frac{\partial U_{xi}}{\partial z} = \left(\frac{{k_{xi}}^2}{k_0}\right)S_{yi} - k_0\sum_p \varepsilon_{i-p} S_{i-p}\,, \tag{8b}$$

or, in a matrix form

$$\begin{bmatrix} \partial \mathbf{S}_y / \partial(z') \\ \partial \mathbf{U}_x / \partial(z') \end{bmatrix} = \begin{bmatrix} \mathbf{0} & \mathbf{I} \\ \mathbf{A} & \mathbf{0} \end{bmatrix}\begin{bmatrix} \mathbf{S}_y \\ \mathbf{U}_x \end{bmatrix}, \tag{9}$$

where $z'=k_0 z$, and $\mathbf{A}=\mathbf{K}_x^2-\mathbf{E}$. By eliminating $\mathbf{U}_x$, equation (9) can be reduced to

$$\left[\partial^2 \mathbf{S}_y / \partial(z')^2\right] = [\mathbf{A}][\mathbf{E}], \tag{10}$$

then the eigenvalue decomposition is able to be carried out more efficiently.

By setting up boundary value conditions of the tangential electric and magnetic field components, the coupled-wave equations can be solved. With the normalized electric-field amplitudes of the reflected wave, reflectivity in each diffraction order can be calculated.

Formulations of rigorous coupled-wave analysis under TM polarization and conical diffraction could be derived in a similar way. Note that during the expansion of permittivity in the coupled-wave equations, the inverse rule should be applied in place of Laurent's rule to achieve a faster convergent result, according to Li's viewpoint[9]. Those formulation details are omitted here.

3. SIMULATIONS AND ANALYSIS

Before introducing the simulation results, it is important to point out that all the structural and optical parameters will affect the convergence to a greater or less degree. We attempted to achieve repeatability and validity of the properties handled here, however, conceivable simulations could hardly be exhausted since the combinations of the parameters are extremely numerous. Multiple simulations have been carried out using different optical and structural parameters, especially the ones in common use, with only a small number of them listed here. Given the generality of the characteristics we observe, both the planar diffraction (TE and TM polarization) and conical diffraction have been taken into account. Consequently, it is considered that the characteristics listed below may be applicable in many cases, at least in a specific range.

3.1 Simulation under varied grating period

By varying the period Λ while fixing other structural parameters (including f and d) and optical parameters (including λ, θ, Φ and ψ), we are able to obtain some meaningful results as shown in Fig. 2. The graph shows that the convergence orders have an approximately linear correlation with the periods. They are fit by linear functions and clearly demonstrated that the convergence orders calculated under different periods are distributed around the linear regression lines. Furthermore, the linear correlations under conical diffraction are not as accurate as those under TM polarization, which is also observed in most of our simulations not listed here.

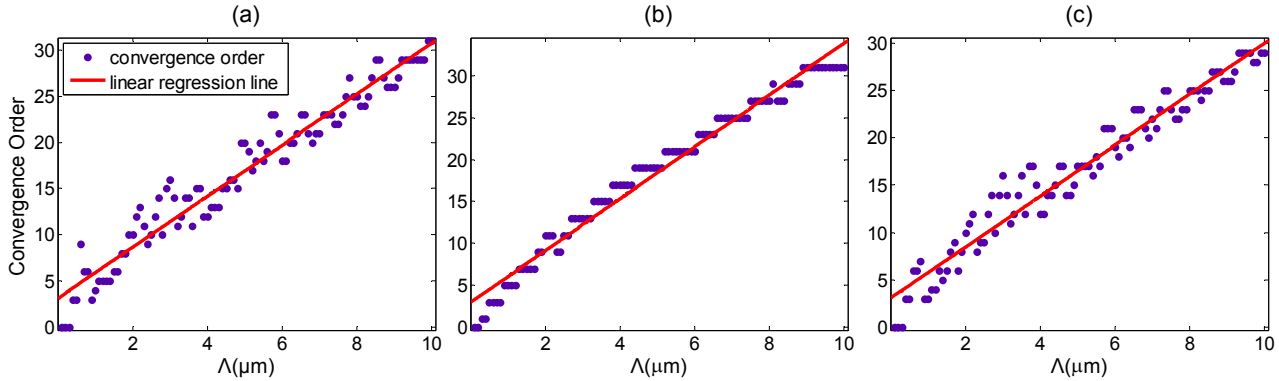

Figure 2. The convergence orders calculated in varied period Λ, while other parameters are fixed in f=0.5, d=0.2μm, λ=0.5μm. (a) TE polarization (θ=10°), (b) TM polarization (θ=10°), and (c) conical diffraction (θ=10°, φ=30°, ψ=45°). The reflectivities calculated with the truncation order of 200 are considered as references, and convergence orders are picked up on an error bound of 0.2%. This indicates that the error corresponding to the reference is no more than 0.2% if any order higher than the convergence order is selected.

Considering the general linearity found above, we performed other simulations with different structural and optical parameters, such as f, d, and θ. For each variable, three values are selected for the test. Influences for conical diffraction are shown in Fig. 3. The results indicate that the linearity exists in vast structures and optical configurations, rather than merely limit to a specific system.

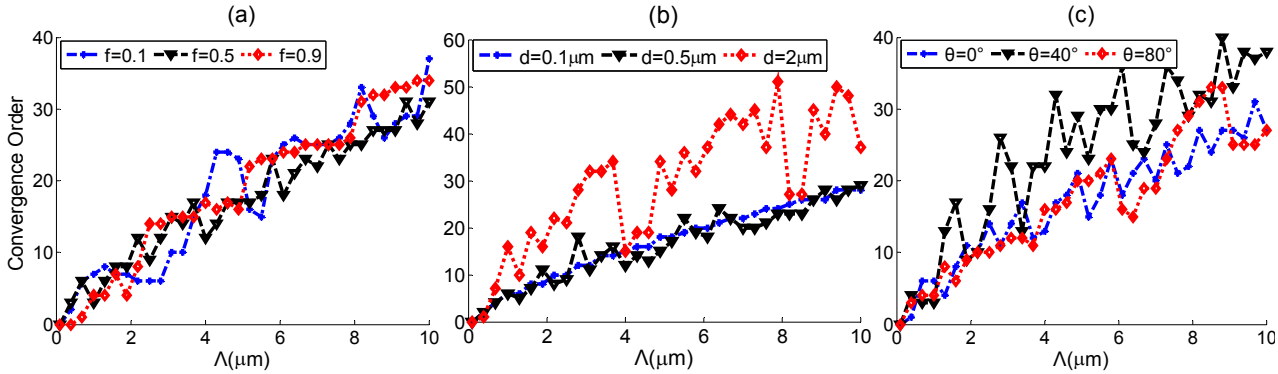

Figure 3. Simulations under (a) varied duty cycle of ridge f, (b) varied depth d, and (c) varied incidence angle θ.

3.2 Simulation under varied illuminated wavelength

In OCD metrology, such as reflectometry and scatterometry, illuminated wavelength can be adjusted in most cases. Therefore, simulations have been carried out by setting up different illuminated wavelengths, with the results shown in Fig. 4. The dash lines are for simulation data and the solid lines for regression. It is noted that the linearity is again nearly independent of the wavelength, and that the illuminated wavelength is intimately related to on the convergence order, when we fix all the structural parameters. With a fixed structure, the convergence order decreases with the growth of wavelength. It is also observed that the slopes of the linear regression lines are dependent on the wavelengths to a great extent, while the intercepts have little correlation with them.

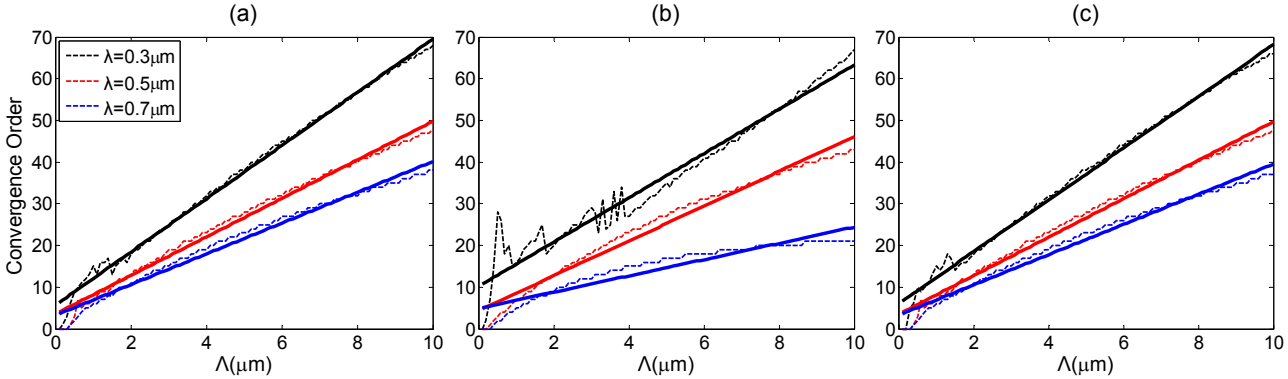

Figure 4. The convergence order calculated for three different wavelengths under (a) TE polarization, (b) TM polarization, and (c) conical diffraction. Other parameters are the same as those listed in Figure 2. The dash and solid lines represent the simulated and the linear regression results respectively.

3.3 Simulation under varied ratio of illuminated wavelength to grating period

We carried out further study and focused on the approximate invariance of the intercepts of different regression lines. The ratio of the illuminated wavelength to the grating period is fixed in the following simulation. The ratio is set to 0.03, 0.1, 0.3,1, and 3 sequentially, with results depicted in different colors in Fig. 5. It is interesting to note that the lower the ratio is, the more order it needs to achieve convergence. When the ratio is set at 3, even the permittivity and electric and magnetic field expanded into zero*th* order can achieve a satisfactory result. The convergence order in each ratio has occupied a limited order range compared to the whole vertical axis. In different ranges of illuminated wavelengths, it can be seen that in the range of 0.5~0.8μm , approximately the visible band, the jump of the convergence order under each ratio varies more slightly than that in the ultraviolet band, which can be observed in TE, TM polarization and conical diffraction. It is thus possible to estimate the order with given structural and optical parameters.

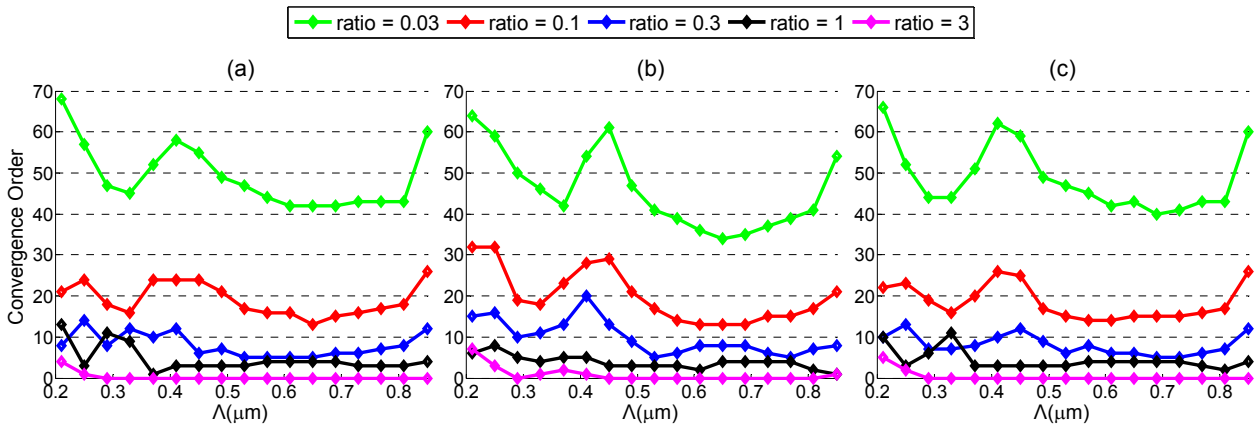

Figure 5. Simulations under different ratios of λ to Λ under(a) TE polarization, (b) TM polarization, and (c) conical diffraction. Other parameters are the same as those listed in Fig. 2. It should be noticed that the grating period is modulation by the fixed ratio, even though the horizontal axis is depicted as the illuminated wavelength.

4. APPLICATION IN ESTIMATION OF THE CONVERGENCE ORDER

From the results shown in Section 3, especially those phenomena observed in Fig. 5, we can estimate the convergence order with given structural and optical parameters. Since the jump in the visible range is slighter than in other ranges, we are more likely to estimate an accurately convergent result for a specific structure. The structural and optical parameters for estimations are listed in Table 1. f is 0.5 in our simulation, and d is fixed at 0.2μm. Assuming that it follows the normal distribution, the 95% confidence interval is calculated through the data in the wavelength range of 0.5~0.8μm. With this confidence interval, an order above the interval has been selected to calculate the reflectivity.

Table 2 shows the results of the estimations. It is noted that the selected order is much less than the reference order (200), especially when the ratio is high. Meanwhile, most of the achieved accuracy is satisfactory, except the 1st sample exceeds the expected error bound of 0.2%. These results thus demonstrate that the estimations carried out here are effective in most cases.

Table 1. Simulation parameters for estimations

Serial Number	λ (μm)	Λ (μm)	Ratio of λ to Λ	Polarization State
1	0.5	16.7	0.03	TE Polarization
2	0.6	6	0.1	TM Polarization
3	0.7	2.33	0.3	TE Polarization
4	0.8	0.8	1	TM Polarization
5	0.5	16.7	0.03	Conical Diffraction
6	0.6	6	0.1	Conical Diffraction
7	0.7	2.33	0.3	Conical Diffraction
8	0.8	0.8	1	Conical Diffraction

Table 2. Results of estimations

Serial Number	μ	σ	Confidence Interval	Selected order	Error
1	43.7	2.0	[42.9, 44.4]	45	0.33%
2	14.5	1.8	[13.9, 15.2]	16	0.01%
3	5.9	0.9	[5.5, 6.2]	7	0.18%
4	3.3	0.8	[3.0, 3.6]	4	0.17%
5	43.1	2.3	[42.2, 44.0]	45	0.07%
6	15.1	1.0	[14.7,15.5]	16	0.09%
7	6.3	1.2	[5.9,6.8]	7	0.07%
8	3.7	0.5	[3.5, 3.9]	4	0.14%

CONCLUSIONS

In this paper, several sets of simulations have been carried out to find out some relationship between the convergence order and the structural or optical parameters for binary rectangular groove gratings. It is observed that the structural dimension and the illuminated wavelength have a combined effect on the convergence order, and the ratio between them could weaken this effect. It is also noticed that in a certain range of wavelength, the jump of convergence order is relatively slight. These observations may provide some guidelines for the estimation of convergence order for a specific sample, and most of the estimations have shown satisfactory accuracy compared to the reference.

ACKNOWLEDGEMENTS

This work was funded by National Natural Science Foundation of China (Grant No. 91023032 and 51005091), Fundamental Research Funds for the Central Universities of China (Grant No. 2010ZD004), and Postdoctoral Science Foundation of China (Grant No. 20100470052).

REFERENCES

[1] Raymond, C., "Overview of scatterometry applications in high volume silicon manufacturing," AIP Conf. Proc. **788**, 394-402 (2005).

[2] Moharam, M. G., Grann, E. B., and Pommet, D. A., "Formulation for stable and efficient implementation of the rigorous coupled-wave analysis of binary gratings," J. Opt. Soc. Am. A **12**(5), 1068-1076 (1995).

[3] Nakata, Y. and Koshiba, M., "Boundary-element analysis of plane-wave diffraction from groove-type dielectric and metallic gratings," J. Opt. Soc. Am. A **7**(8), 1494-1502 (1990).

[4] Ichikawa, H., "Electromagnetic analysis of diffraction gratings by the finite-difference time-domain method," J. Opt. Soc. Am. A **15**(1), 152-157 (1998).

[5] Raymond, C. J., Littau, M., Chuprin, A. and Ward, S., "Comparison of solutions to the scatterometry inverse problem," Proc. SPIE **5375**, 564-575 (2004).

[6] Lee, W. and Degertekin, F. L., "Rigorous coupled-wave analysis of multilayered grating structures," J. Lightwave Technol. **22**(10), 2359-2363 (2004).

[7] Chu, H., "Finite difference approach to optical scattering of gratings," Proc. SPIE **5188**, 358-370 (2003).

[8] Moharam, M. G., Grann, E. B. and Pommet, D. A., "Stable implementation of the rigorous coupled-wave analysis for surface-relief gratings: enhanced transmittance matrix approach," J. Opt. Soc. Am. A **12**(5), 1077-1086 (1995).

[9] Li, L., "Use of Fourier series in the analysis of discontinuous periodic structures," J. Opt. Soc. Am. A **13**(9), 1870-1876 (1996).